THE ROYAL SOCIETY

X-ray topographic observation of magnetic domain structures induced by stresses

By Milena Polcarová[1], Jaroslav Brádler[1], Ivan Tomáš[1], Alain Jacques[2] and Amand Georges[2]

[1]*Institute of Physics AS CR, Na Slovance 2, 182 21 Prague 8, Czech Republic*
[2]*Laboratoire de Physique des Matériaux, Ecole des Mines, Parc de Saurupt, 54042 Nancy, France*

Magnetic domain structures were observed by synchrotron radiation back-reflection topography in bicrystals of Fe–4at%Si. Their appearance depends on the type of the bicrystal, on the inspected surface and on the applied stress. Models of the probable domain structures were suggested and topographic contrast explained.

Keywords: X-ray topography; magnetic domains; back reflection

1. Introduction

X-ray diffraction topography has been used by many authors for investigation of magnetic domain structures. It has been shown that the magnetostrictive deformation is the reason of the visibility of domains (Polcarová & Lang 1962). The contrast appears due to variation of distortion at the domain walls. The 90° walls in Fe–Si are visible if $\boldsymbol{g}\cdot(\boldsymbol{m}_2-\boldsymbol{m}_1)\neq 0$, where $\boldsymbol{g}$ is the diffraction vector and $\boldsymbol{m}_1, \boldsymbol{m}_2$ are unit vectors parallel to the magnetization in the domains connected by the wall (Polcarová & Kaczér 1967). The 180° walls are only slightly visible as a result of the surface relaxation of the stresses inside the wall (Lang & Polcarová 1991). The surface stress relaxation is also important for the contrast formation due to wall junctions and other more complicated structures (Kléman *et al*. 1978; Lejček 1978). Contrast on the 90° walls was calculated using the dynamical theory of X-ray diffraction and good agreement with the experiments was found (Polcarová & Brádler 1982). If a sufficiently sensitive experimental setting is applied, the tilt of the diffracting planes at the wall can be measured directly (Brádler & Polcarová 1972). Images of wall junctions and other more complicated structures were successfully simulated (Kléman *et al*. 1978). Good understanding of the contrast formation is necessary for the interpretation of topographic images.

Changes of magnetic domain structures induced by an external magnetic field or by stresses were also followed by X-ray topography (Labrune & Kléman 1974; Brádler & Polcarová 1978; Stephenson *et al*. 1980; Dudley & Miltat 1989). Most experiments were done on thin plates with (100) or (110) surface where the domain structure was relatively simple even if the stress was applied.

In the following, observation of surface domain structures in bulk specimens of Fe–4at%Si bicrystals is described. Both tension and compression stresses were applied along well-defined crystallographic directions. Synchrotron radiation (SR) reflection topography was used to inspect surfaces of ($hk0$) type.

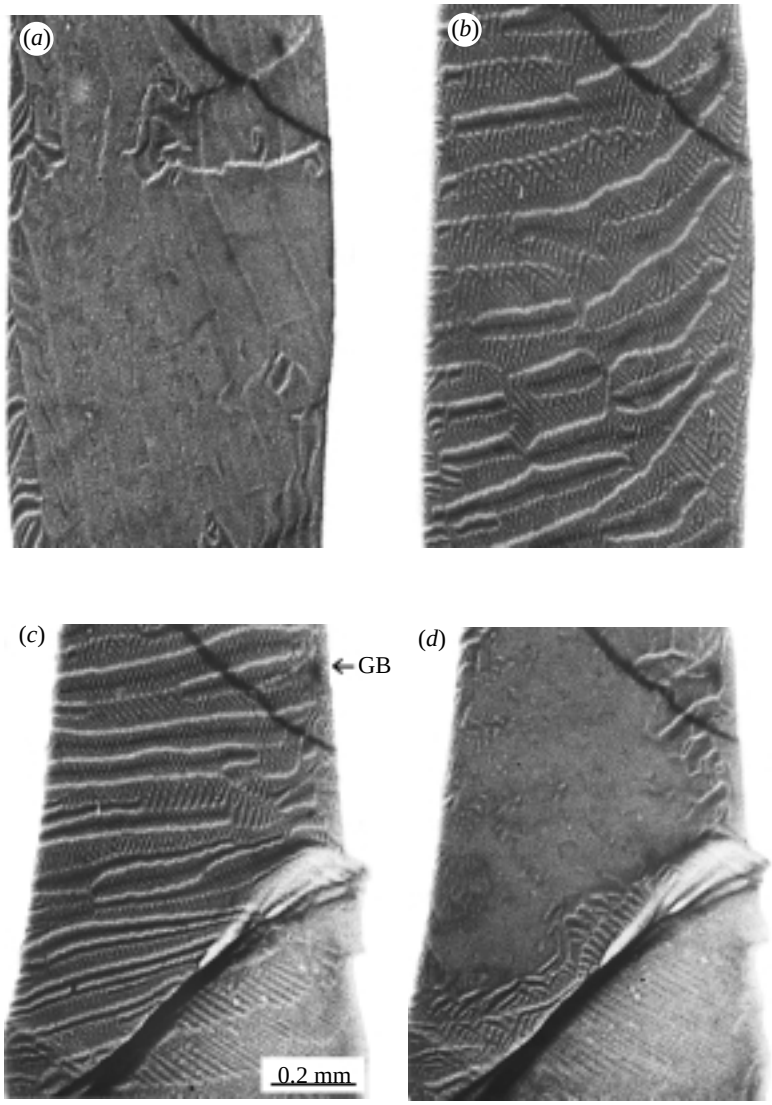

Figure 1. Parts of topographs of the grain B of a $\Sigma 9$ bicrystal deformed by tension with white-beam synchrotron radiation, symmetrical back reflection on (110) planes, Bragg angle 65° (several orders of diffraction contribute to the image), specimen thickness 0.35 mm and stress magnitudes, σ of (*a*) 17 MPa; (*b*) 265 MPa; (*c*) 206 MPa; (*d*) 22 MPa.

2. Experiments

The bicrystals with required parameters were grown in the Institute of Physics, Prague in order to study the interaction of slip dislocations with grain boundaries (GBs) during the initial stage of plastic deformation. Specimens of special shape were prepared to fit into the deformation stage developed in Ecole des Mines, Nancy. SR reflection topography was carried out in LURE, Orsay, and in ESRF, Grenoble. Symmetric reflection from planes parallel to the surface and white or monochromatic beam and specimen rocking were used. The topographs were taken under gradually

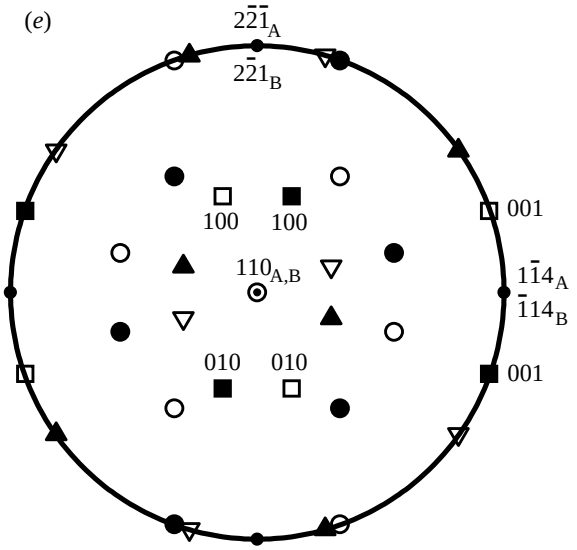

Figure 1. (*Cont.*) Orientation of the topograph is shown by the stereographic projection (*e*). Directions in the grain A and B are given by the solid and open symbols, respectively.

increasing stress and registered on Ilford L4 plates (for experimental details, see Polcarová *et al*. 1998, 1999).

In addition to images of crystal defects like subgrain boundaries, surface imperfections and slip bands, images of magnetic domains can also be seen in the topographs. Their appearance varies with the type of bicrystal, with the investigated surface and with the sign and magnitude of the applied stress.

$\Sigma 9$ bicrystals† can be described by rotation around the [110] direction by an angle 38.94°. The GB plane is $(1\bar{1}4)_A = (\bar{1}14)_B$, the external force is applied along the $[2\bar{2}\bar{1}]_A = [2\bar{2}1]_B$ direction, the inspected surface is the $(110)_{A,B}$ plane. If no stress is applied, no magnetic domains are visible. The domain pattern appears with application of a tensile stress, and it becomes finer and more complicated when the stress is increased. The white and black lines indicating positions of the surface domains form more or less regular structure. After the stress is relaxed most of the domain images disappear again (figure 1). Compression stress does not induce any visible domains.

The grains of $\Sigma 3$ bicrystals are mutually rotated by an angle of 70.53° around the [110] direction. The GB plane is $(1\bar{1}2)_A = (\bar{1}12)_B$, the external force is applied along the $[152]_A = [15\bar{2}]_B$ direction, the inspected surface is the $(20\bar{1})_A = (201)_B$ plane. No magnetic domains are visible when zero stress or tensile stress is applied. Complicated domain structures appear in compression, however (figure 2).

† Macroscopic geometrical characterization of GB is specified by five parameters associated with the misorientation relation between the crystals (grains) and the orientation of the interface normal. A superlattice constructed by coinciding atom positions of the crystal lattices of both adjacent grains when they are extrapolated across the boundary to penetrate each other is called coincidence site lattice (CSL). The ratio of the volume of the CSL unit cell to the volume of the lattice unit cell is denoted Σ and is often used as a geometrical parameter characterizing the structure/property relationship.

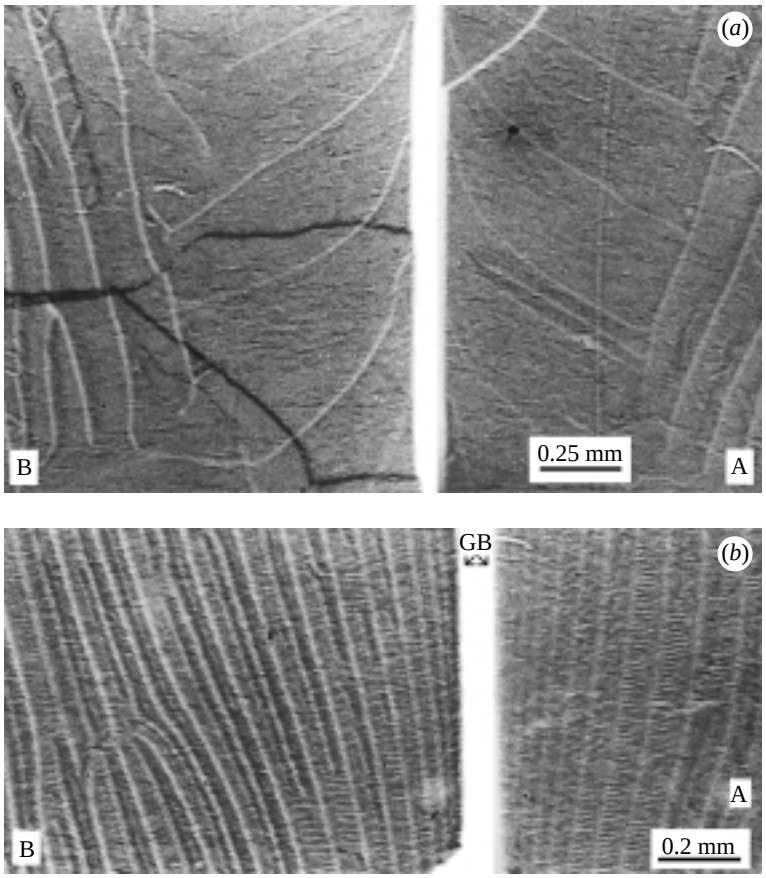

Figure 2. Parts of topographs of both grains of a $\Sigma 3$ bicrystal deformed by compression with monochromatic beam synchrotron radiation ($\lambda = 0.105$ nm, symmetrical 402 back reflection, Bragg angle 55°, specimen thickness 4 mm and stress magnitudes, σ, of (a) -1.2 MPa and (b) -126 MPa.

3. Domain structures

(a) *Domain formation*

Magnetic domain structure appears in ferromagnetic samples in order to optimize the exchange and magnetostatic energy contributions. The actual size and shape of domains is strongly coupled with magnetic non-uniformities (the sample surfaces being usually the most important of all) and it is influenced by magnitudes and geometry of the magnetocrystalline and magnetoelastic anisotropy.

The qualitative description of the probable domain structure in the investigated samples is based on the following.

(i) *Sample parameters*: bulk bicrystals described above, sample thickness much greater than $\sqrt{A/K}$, where A is the exchange stiffness constant, K is the first cubic anisotropy energy coefficient and $\sqrt{A/K}$ is the domain wall width parameter. The thick bulk sample means that large magnetic domains can be expected within the specimen volume, whereas—in case that no easy axis of

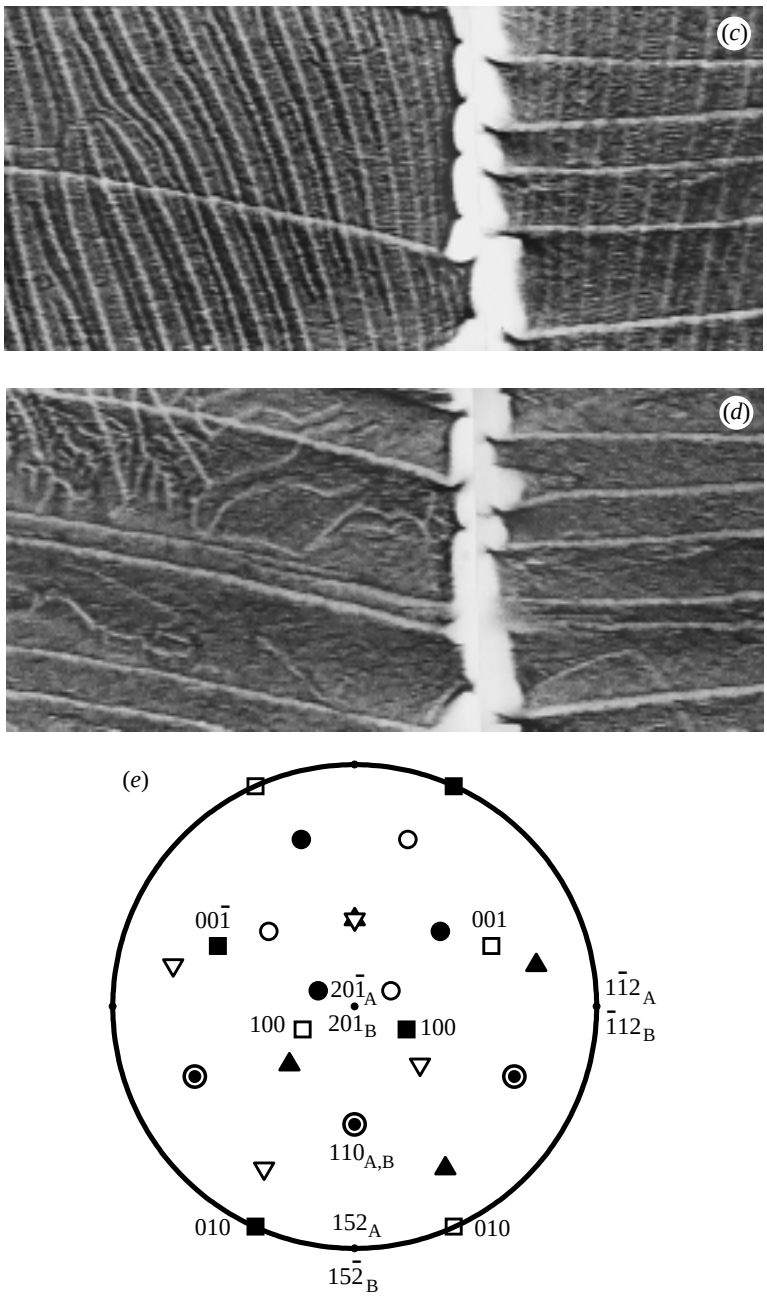

Figure 2. (*Cont.*) (*c*) −144 MPa; (*d*) −0.5 MPa. Orientation of the topograph is shown by the stereographic projection (*e*), directions in the grain A and B are given by solid and open symbols, respectively.

magnetization lies in the inspected surface—branching of domains into complicated patterns appears close to the surface.

(ii) *Material parameters*: cubic anisotropy, $K > 0$, $K_d \gg K$, where $K_d = J_S^2/2\mu_0$

is the demagnetization energy coefficient, J_S is the saturation magnetic polarization (magnetization) and μ_0 is the permeability of vacuum. The condition $K_d \gg K$ means that no open-flux domain structure or 'magnetically charged' domain walls can be expected. The structure will be closed and the normal component of the magnetization vector will have the same magnitude at both sides of any domain wall.

The crystalline cubic anisotropy energy density is expressed by the formula

$$E_C = K(\alpha_1^2\alpha_2^2 + \alpha_1^2\alpha_3^2 + \alpha_2^2\alpha_3^2)$$

and α_i are direction cosines of the magnetization with respect to the cubic axes. The condition $K > 0$ means that the crystallographic axes [100], [010], [001] are the mutually equivalent easy magnetization directions in the unstressed samples. We assume the applied stress to be small enough to keep these directions to be *locally* the easiest ones even if the stress is present, and to keep the magnetization vector inside each domain *parallel* to one of the cubic axes (i.e. α_i can be 0 or 1 only). However, we assume the applied stress to be large enough as to *cancel* the mutual *equivalency* of the cubic axes, because the contributions of the magnetoelastic energy along each of the three axes can be different.

(iii) *Stress parameters*: the magnetoelastic energy density can be expressed by the formula (Hubert & Schaefer 1998)

$$E_{ME} = -\tfrac{3}{2}\lambda_{100}\sigma(\alpha_1^2\gamma_1^2 + \alpha_2^2\gamma_2^2 + \alpha_3^2\gamma_3^2) - 3\lambda_{111}\sigma(\alpha_1\alpha_2\gamma_1\gamma_2 + \alpha_2\alpha_3\gamma_2\gamma_3 + \alpha_3\alpha_1\gamma_3\gamma_1),$$

where λ_{100} and λ_{111} are the magnetostriction constants in the $\langle 100\rangle$ and $\langle 111\rangle$ directions, and $\sigma_{ij} = \sigma\gamma_i\gamma_j$ are the stress tensor components; σ is positive for tension and negative for compression.

For the applied stress direction in the $\Sigma 9$ bicrystal we have $\gamma_1^2 = \gamma_2^2 = 0.444$ and $\gamma_3^2 = 0.111$. Therefore, at tension ($\sigma > 0$) the magnetoelastic energy is minimum if $\alpha_3 = 0$ and α_1 or $\alpha_2 = 1$, i.e. if the magnetization is parallel either to the $\pm[100]$ or $\pm[010]$ directions. At compression the energy is minimum for magnetization direction $\pm[001]$, i.e. the cubic direction parallel to the surface.

In the $\Sigma 3$ bicrystal, $\gamma_1^2 = 0.033$, $\gamma_2^2 = 0.832$ and $\gamma_3^2 = 0.133$. In tension the minimum is for the direction $\pm[010]$ parallel to the surface, in compression for the direction $\pm[100]$.

From the material and sample parameters it can be generally concluded that large magnetic domains magnetized along the magnetically easiest crystallographic directions will be found in the bulk of the samples. If the easiest direction does not lie in the inspected surface plane, the bulk domains cannot penetrate up to this surface and are supplemented by closure domains magnetized along a next possible easiest direction.

(*b*) $\Sigma 9$ *bicrystal*

In the unstressed sample, $\sigma = 0$, all the cubic directions are equivalent to one another and the [001] lies in the observed (110) surface. As a consequence, a domain

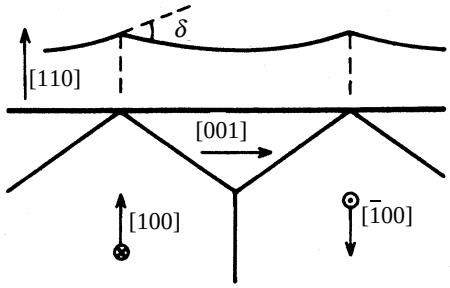

Figure 3. Model of the low-stress domain structure in grain B of the $\Sigma 9$ bicrystal: section ($\bar{1}10$) perpendicular to the (110) surface. The 90° walls between the bulk and the closure domains are parallel to the {111} planes and the angle with the surface is 35.3°. In the upper part of the figure the tilt of the surface planes is sketched.

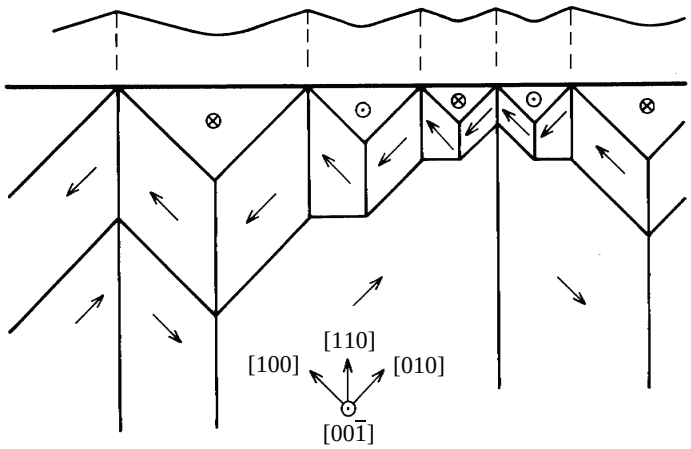

Figure 4. Model of the high-stress domain structure in grain B of the $\Sigma 9$ bicrystal: (001) section perpendicular to the (110) surface. In the upper part of the figure the tilt of the surface planes is sketched.

structure of bulk slabs magnetized alternatively along [001] and [00$\bar{1}$] directions is formed with no closure domains at the surface.

If a low tensile stress is applied, a domain structure of slabs perpendicular to the [001] direction magnetized alternatively along ±[100] and/or ±[010] directions is formed in the bulk of the sample. Surface closure domains magnetized in the ±[001] directions close the magnetic flux. Figure 3 shows a section in the ($\bar{1}10$) plane perpendicular to the sample surface. The pattern resembles the classical Landau–Lifshitz structure (Hubert & Schaefer 1998) but for the angle of magnetization in the slab domains making 45° with the plane of the drawing. The walls between the slabs and the closure domains are parallel to the {111} planes. As they are free to tilt around the direction $\boldsymbol{m}_2 - \boldsymbol{m}_1$, however, their intersection with the surface can be wavy (see figure 1*a*).

At higher tensile stress the differences between the magnetic easiness of the cubic directions are increased, the extra magnetoelastic energy of the large volumes of the closures magnetized along [001] is no longer acceptable, and the domain structure is

changed in order to decrease it. A new structure of slabs parallel to the [001] direction magnetized along the two easiest directions appears in the bulk. The magnetic flux is closed by closure domains magnetized along the ±[001]. The final equilibrium of the domain structure is achieved by decreasing the total volume of the disadvantageously magnetized closure domains. This is made possible by branching of the domain structure close to the surface, which is paid for by an increase of the total wall area. The result is that a fine branching of the surface domain structure is observed with the increasing magnitude of the applied stress, but the bulk inside of the sample remains magnetized along the two magnetically easiest axes in large slabs with large period. One of the possible models of this structure is drawn in figure 4. Inside the specimen it consists of domains magnetized in ±[100] and ±[010] directions with 90° walls between them. This model resembles that shown in the book of Hubert & Schaefer (1998). An alternative structure formed by domains magnetized along only one of the easy directions in the bulk with 180° walls was suggested by Corner & Mason (1964).

With increasing stress magnitude, a still more complicated structure appears. It is periodic in two or even in three directions and it can be described as a combination of the two former cases (Hubert & Schaefer 1998). Thus the total volume of the closure domains decreases at the penalty of larger total area of the domain walls.

The last topograph of this series was taken after the external stress was reduced to a low value (figure 1*d*). As the specimen was plastically deformed, however, inhomogeneous internal stresses became present in the sample, in the neighbourhood of the slip bands in particular. Therefore, although most of the complicated domain structures disappeared, some remained visible, similar to those seen in the topographs taken under large external stress.

If compression stress is applied, the easiest magnetic direction is [001]. As it lies in the observed (110) surface, the domain structure remains the same as in the unstressed sample.

(*c*) $\Sigma 3$ *bicrystal*

The same reasoning for the suggestion of the models of the domain structures is valid in this case as for the $\Sigma 9$ bicrystals. Here, however, the two local magnetization easy directions non-parallel to the inspected surface are not equivalent to each other and are also not symmetrical with respect to the surface.

Without external stress, a domain structure of bulk slabs magnetized alternatively along the [010] and [0$\bar{1}$0] directions is formed in the sample, with no closure domains at the surface. The 180° Bloch walls penetrate up to the surface.

If tensile stress is applied, the easiest magnetic direction is [010]. As it lies in the observed (201) surface, the domain structure remains the same as in the unstressed sample.

Under compressive stresses the easiest direction of magnetization is [100]. The simplest domain structure consists of slabs perpendicular to the [010] axis and magnetized alternatively along the [100] and [$\bar{1}$00] directions. They are formed in the bulk of the sample and completed by closure domains magnetized in the ±[010] directions (figure 5). This structure is similar to that in figure 3, but the angle between the [100] direction and the plane of the drawing is 26.57° and the wall planes between the slabs and closure domains are {221}.

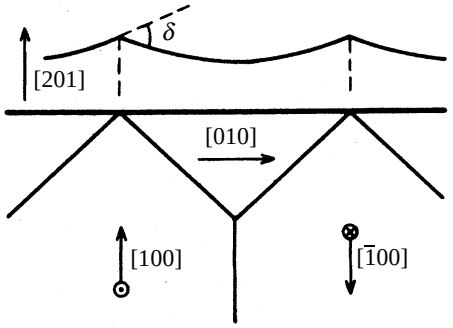

Figure 5. Model of the low-stress domain structure in grain B of the $\Sigma 3$ bicrystal: section $(10\bar{2})$ perpendicular to the (201) surface. The 90° walls between the bulk and the closure domains are parallel to the {221} planes and the angle with the surface is 41.8°. In the upper part of the figure the tilt of the surface planes is sketched.

In the case of larger compressive stress a domain structure analogous with that in the $\Sigma 9$ bicrystal is formed, but the bulk slabs are magnetized in the easiest direction $\pm$[100] only (figure 6). Near the surface, branching of the slabs occurs with the help of the second easiest direction $\pm$[001]. Fine surface domains $\pm$[010] close the magnetic flux.

When the magnitude of the compressive stress grows further, the total volume of the closure domains magnetized along the most difficult of the local easy axes [010] is decreased in the domain system periodic in two mutually perpendicular directions, i.e. a combination of the two mentioned cases (Hubert & Schaefer 1998). Figure 2*a* shows the first appearance of such a three-dimensional domain structure, where the applied stress brings about just the very beginning of the [010] closure domain periodicity along the second direction. Branching of the surface domain structure increases with increasing values of the compressive stress.

After relaxation of the external stress, all domains disappeared in the shown part of grain A, whereas remainders are present in grain B (figure 2*d*). This observation can be explained as follows. The density of the slip bands is higher in grain A than in grain B, i.e. grain A is *plastically* deformed more than grain B. As a result of the mutual influence of the two grains, grain A is *elastically* elongated and grain B *elastically* compressed. This agrees with our observation that the complicated domain structure appears only under compression stress.

4. Diffraction contrast

The image of the domain structures in the topographs (figures 1 and 2) is mainly formed by the orientation contrast. This was confirmed by the observation that the width of the white and black stripes increases with the distance of the photographic plate from the specimen.

The white stripes can be explained by a tilt of the diffracting planes near the lines where the 90° walls emerge to the surface. The distortion of the planes near the surface was calculated by Lejček (1978) for the Landau–Lifshitz domain structure and experimentally confirmed by Brádler & Polcarová (1978). It is caused by surface relaxation of the stresses due to the row of 90° wall junctions placed near the free surface. The tilt of the surface planes is proportional to the magnetostriction

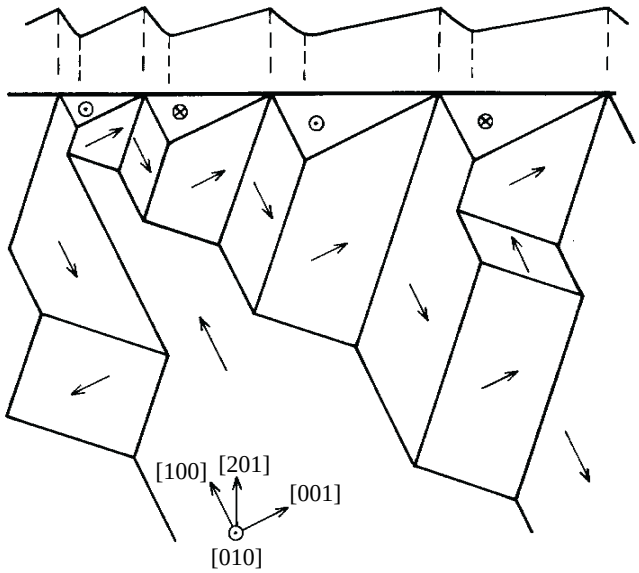

Figure 6. Model of the high-stress domain structure in grain B of the $\Sigma 3$ bicrystal: (010) section perpendicular to the (201) surface. In the upper part of the figure the tilt of the surface planes is sketched.

constant λ_{100} ($\delta \simeq 17''$). Our model for $\Sigma 9$ specimens (figure 3) differs from that of Landau–Lifshitz: the two magnetization directions do not lie in the plane perpendicular to the walls and the 90° walls are parallel to the {111} planes. The tilt of the diffracting (110) planes due to {111} 90° walls calculated according to Polcarová & Gemperlová (1969) is $\delta \approx 6''$. A similar result can be expected for the $\Sigma 3$ specimens with calculated tilt $\delta \approx 11''$ (figure 5).

The surface distortion due to the models shown in figures 4 and 6 is more complicated as it is a three-dimensional problem. It has not been solved analytically. By analogy with the above-mentioned case, we can estimate the surface plane bending as sketched in the upper parts of figures 4 and 6. At lines where the 90° walls emerge on the surface, a tilt of the plane similar to that in the models in figures 3 and 5 is highly probable. A white stripe will appear on the topograph through the orientation contrast, i.e. as a gap between the images of the neighbouring regions.

Black stripes appear in the images of domain structures in figures 1 and 2, which are interpreted by the models in figures 4 and 6. They are also due to the orientation contrast, this time to the superposition of the images. This can be explained only by a tilt of surface planes opposite to that forming the white stripes. Such a tilt can be due to surface relaxation of stresses connected with the line of junction of three 90° walls at the bottom of the closure domains. This explanation is supported by the following observations. The black stripes are placed symmetrically between the white stripes in the topographs of $\Sigma 9$ samples, and asymmetrically in $\Sigma 3$ samples in agreement with the models. They are placed symmetrically with respect to the grain boundary in the grains of the $\Sigma 3$ specimen as it corresponds to the symmetry of the bicrystal. They are narrower and more pronounced when the domains are smaller and denser and in the large domains they are not visible at all.

The 180° walls are not visible in the present experimental setting.

5. Conclusions

(i) Complicated magnetic domain structures arise at the (110) and (201) surfaces of two different bicrystals of Fe–4at%Si under external tensile and compressive stresses applied along definite crystallographic directions.

(ii) Models of the structures based on the general principles of the domain structure formation and on the particular geometrical, material and stress parameters of the samples were constructed to interpret the topographic images. They correspond very well with the expected stress-induced relative non-equivalency of the cubic axes within the whole range of the applied tensile and compressive stress.

(iii) Stresses due to the wall junctions at the closure domains relax on the free surface. Resulting distortion of the surface planes is the reason for orientation contrast formation.

(iv) The residuals of the special domain structures observed after the stress relaxation give well-marked evidence about the existence and sign of the internal stresses present in the specimens due to the plastic deformation.

The financial supports by the Grant Agency of the Czech Republic (the contracts no. 202/98/1281 and no. 101/99/1662) and by PICS (no. 477) are appreciated.

References

Brádler, J. & Polcarová, M. 1972 Study of magnetostrictive deformation of Fe–Si by X-rays. *Physica Status Solidi* A **9**, 179–186.

Brádler, J. & Polcarová, M. 1978 X-ray topographic investigation of surface distortion due to a magnetic domain structure in strained Fe–Si crystals. *Acta Crystallogr.* A **34**, S251.

Corner, W. D. & Mason, J. J. 1964 The effect of stress on the domain structure of Goss textured silicon–iron. *Br. J. Appl. Phys.* **15**, 709–718.

Dudley, M. & Miltat, J. 1989 Synchrotron topographic studies of the effects of elastic stress on magnetic domain configurations in Fe–3.5wt%Si single crystals. *Nucl. Instrum. Meth.* B **40/41**, 393–397.

Hubert, A. & Schaefer, R. 1998 *Magnetic domains—the analysis of magnetic microstructures*, 1st edn, pp. 6, 138, 342. Springer.

Kléman, M., Labrune, M., Miltat, J., Nourtier, C. & Taupin, D. 1978 Magnetostriction and magnetostrictive effects in magnetic materials. *J. Appl. Phys.* **49**, 1989–1991.

Labrune, M. & Kléman, M. 1974 Study of magnetic structures induced by bending in (100) Fe–Si single crystals. *J. Appl. Phys.* **45**, 2716–2723.

Lang, A. R. & Polcarová, M. 1991 X-ray topographic observation of 180° domain walls in (001) plates of nearly perfect iron–silicon alloy single crystals. *Phil. Mag. Lett.* **63**, 225–231.

Lejček, L. 1978 Magnetostrictive displacements at the surface due to domain wall junctions. *Czech. J. Phys.* B **28**, 434–441.

Polcarová, M. & Brádler, J. 1982 Theoretical and experimental study of the diffraction contrast on magnetic domain walls. *Z. Naturf.* A **37**, 419–426.

Polcarová, M. & Gemperlová, J. 1969 Distortion of an Fe–Si single crystal and X-ray topographic contrast due to a 90° ferromagnetic domain wall. *Physica Status Solidi* **32**, 769–778.

Polcarová, M. & Kaczér, J. 1967 X-ray diffraction contrast on ferromagnetic domain walls in Fe–Si single crystals. *Physica Status Solidi* **21**, 635–642.

Polcarová, M. & Lang, A. R. 1962 X-ray topographic studies of magnetic domain configurations and movements. *Appl. Phys. Lett.* **1**, 13–15.

Polcarová, M., Gemperlová, J., Brádler, J., Jacques, A., George, A. & Priester, L. 1998 *In situ* observation of plastic deformation of Fe–Si bicrystals by white-beam synchrotron radiation topography. *Phil. Mag.* A **78**, 105–130.

Polcarová, M., Brádler, J., Gemperlová, J., Jacques, A. & George, A. 1999 SR topography of plastically deformed Fe–Si bicrystals. *J. Phys.* D **32**, A109–A113.

Stephenson, J. D., Tuomi, T. & Kelhä, V. 1980 Stress-induced magnetization in a (100) [001] Fe–3wt%Si polycrystal influenced by a [100] magnetic field. *Physica Status Solidi* A **57**, 191–202.